

Controllable Synthesis of Platinum-Tin Intermetallic Nanoparticles with High Electrocatalytic Performance for Ethanol Oxidation

Qian Di^a, Xixia Zhao^a, Wenjing Zhu^b, Yiliang Luan^e, Zhen Hou^d, Xiaokun Fan^d, Yan Zhou^b, Shutao Wang^c, Zewei Quan^d, Jun Zhang^{*a, b}

^a State Key Laboratory of Heavy Oil Processing, College of Chemical Engineering, China University of Petroleum, Qingdao, Shandong 266580, P. R. China.

^b School of Materials Science and Engineering, China University of Petroleum (East China), Qingdao, Shandong 266580, P. R. China.

^c College of Science, China University of Petroleum (East China), Qingdao, Shandong 266580, P. R. China.

^d Department of Chemistry, Southern University of Science and Technology (SUSTech), Shenzhen, Guangdong 518055, P. R. China.

^e First-year Research Immersion, State University of New York at Binghamton, NY, 13902

Supplementary Figures and Tables:

Table S1 Products under different feeding amounts of SnCl₂, mole ratio values of precursors between Pt and Sn, and volume of OAc are listed.

SnCl ₂ / mg	Pt: Sn (mole ratio)	OAc/ ml	Product
0	1: 0	0	Pt
4	1: 0.415	0	Pt ₃ Sn
10	1: 1.04	0	PtSn
15	1: 1.56	0	PtSn
20	1: 2.07	0	PtSn ₂
30	1: 3.11	0	PtSn ₂
40	1: 4.15	0.250	PtSn ₄

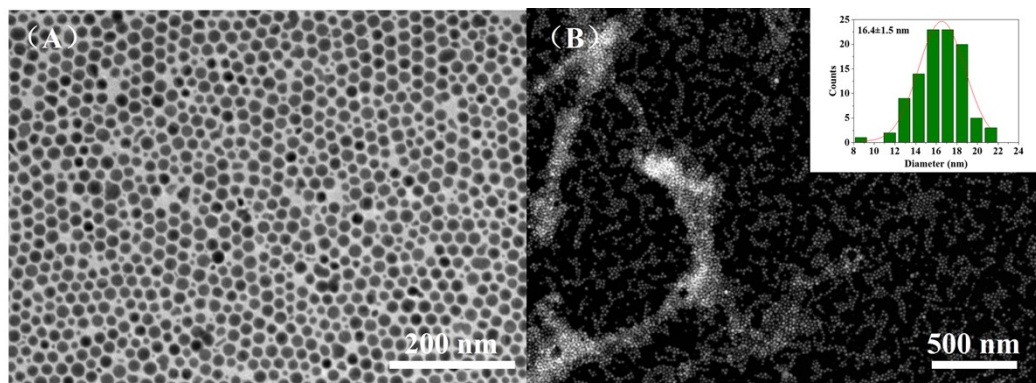


Fig. S1 (A) TEM and (B) High-angle annular dark-field image (HAADF) of PtSn₄. The inset figure is the histogram of the particle size distribution curve of PtSn₄.

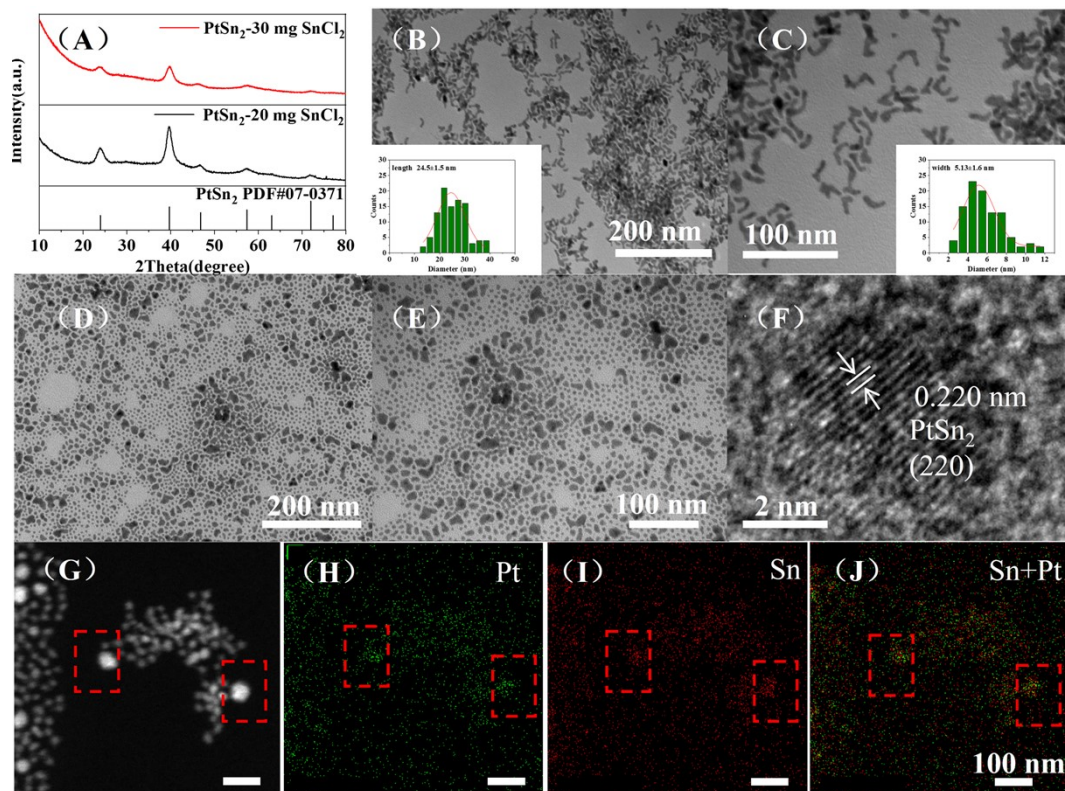


Fig. S2 Morphology and structure characterization of PtSn₂. (A) XRD, (B-E) TEM, (F) HRTEM, and (G-J) EDS elemental mapping patterns of PtSn₂ under different feeding amounts of SnCl₂. 20 mg of SnCl₂ is added for (B-C); 30 mg of SnCl₂ is added for (D-J). The inset figures in (B) and (C) are the histograms of the length and width of PtSn₂, respectively. The scale bar of the figure (G-I) is the same as that of the figure (J).

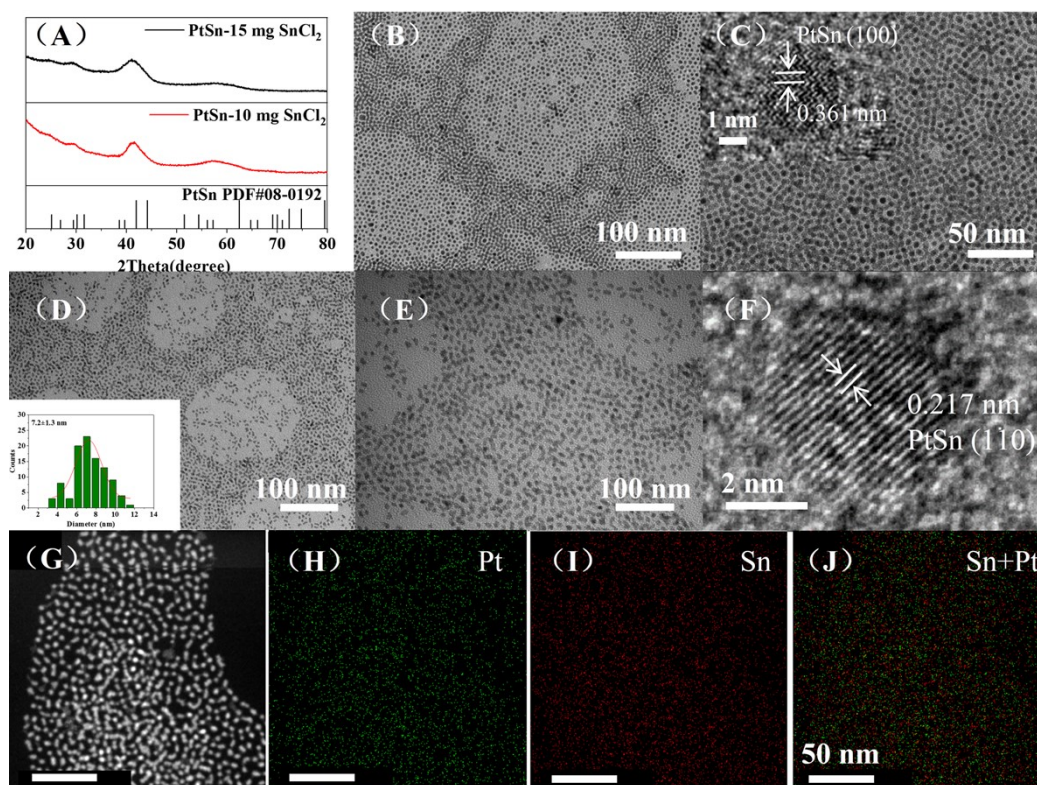


Fig. S3 Morphology and structure characterization of PtSn. (A) XRD, (B-E) TEM, the inset figure in (C) and (F) HRTEM, and (G-J) EDS elemental mapping patterns of PtSn under different feeding amounts of SnCl_2 . 10 mg of SnCl_2 is added for (B-C); 15 mg of SnCl_2 is added for (D-J). The inset figure in (D) is the histogram of the particle size distribution curve of PtSn. The scale bar of the figure (G-I) is the same as that of the figure (J).

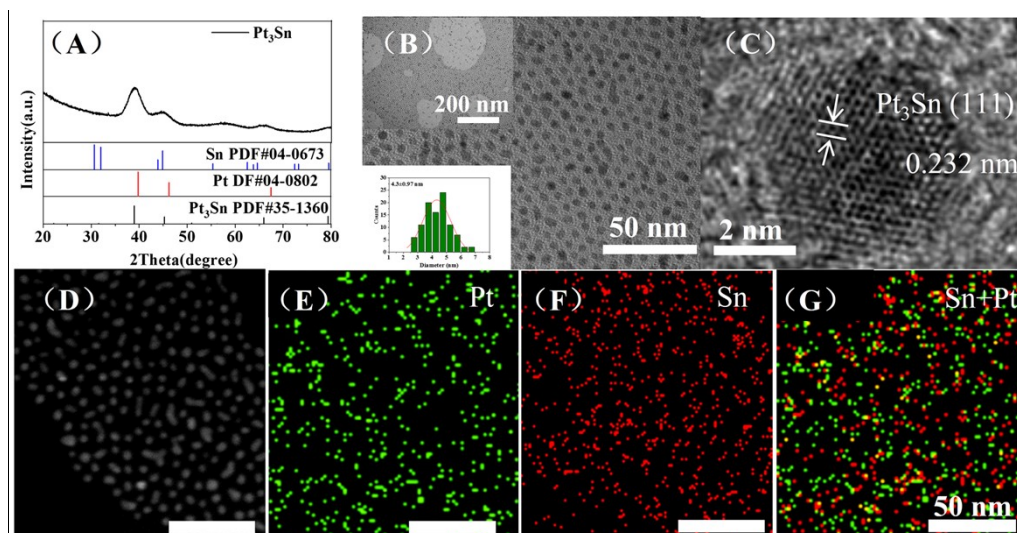


Fig. S4 Morphology and structure characterization of Pt₃Sn. (A) XRD, (B) TEM, (C) HRTEM, and (D-G) EDS elemental mapping patterns of Pt₃Sn under the feeding amounts of 4 mg of SnCl₂. The scale bar of the figure (D-F) is the same as that of the figure (G). The inset figure in (B) is the TEM image and histogram of the particle size distribution curve of Pt₃Sn.

Table S2 Mole ratio value between Pt and Sn in EDS results. (10 mg of SnCl₂ is added for PtSn, 20 mg of SnCl₂ is added for PtSn₂).

EDS	Sn	Pt
Pt ₃ Sn	0.712	1
PtSn	1.14	1
PtSn ₂	2.44	1
PtSn ₄	4.68	1

Table S3 Conditions of control experiment. The names and their corresponding conditions are listed.

Control experiments	Temperature	Chemical agents	Results
PtSn ₄ without HMDS-control experiment	220 °C	SnCl ₂ (40 mg), Pt(acac) ₂ , OAm, ODE, OAC, W(CO) ₆	NO Sn, Pt or Pt _x Sn _y
PtSn ₂ without HMDS control experiment	220 °C	SnCl ₂ (20 mg), Pt(acac) ₂ , OAm, ODE, W(CO) ₆	NO Sn, Pt or Pt _x Sn _y
Pt HMDS controlled experiment	220 °C	HMDS, Pt(acac) ₂ , OAm, ODE, OAC, W(CO) ₆	ca. 5 nm Pt nanoparticles
Pt without HMDS-control experiment	220 °C	Pt(acac) ₂ , OAm, ODE, OAC, W(CO) ₆	ca. 5 nm Pt nanoparticles
Sn HMDS control experiment	220 °C	HMDS, SnCl ₂ (40 mg), OAm, ODE, OAC, W(CO) ₆	ca. 20 nm Sn nanoparticles
Sn without HMDS control experiment	220 °C	SnCl ₂ (40 mg), OAm, ODE, OAC, W(CO) ₆	SnO _x (x=1,2) nanoparticles

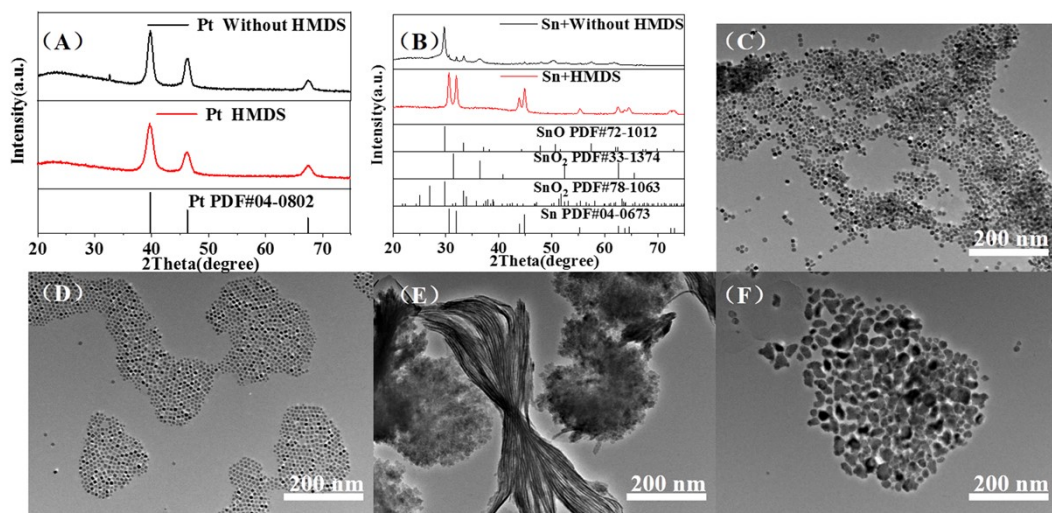


Fig. S5 XRD (A-B) and TEM (C-F) patterns of Pt and Sn in the control experiment. (A, C, D) Pt control experiment (C) without HMDS or (D) with HMDS. (B, E, F) Sn control experiment (E) without HMDS or (F) with HMDS.

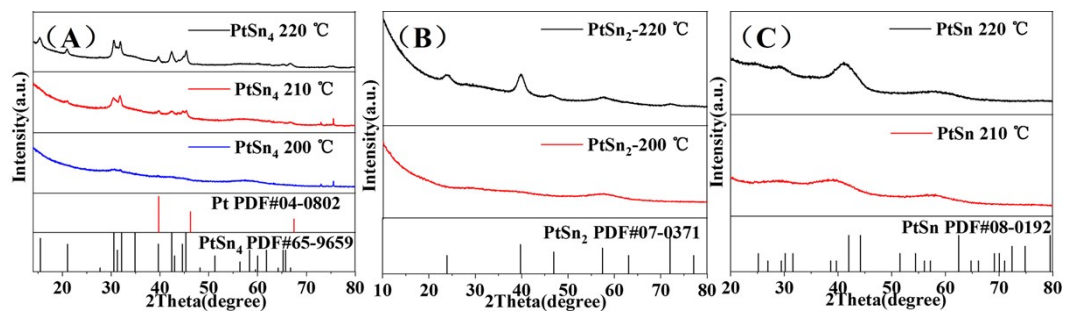


Fig. S6 XRD patterns of Pt_xSn_y in the temperature-dependent experiment. (A) $PtSn_4$, (B) $PtSn_2$ and (C) $PtSn$. 40 mg, 30 mg and 15 mg of $SnCl_2$ is added for $PtSn_4$, $PtSn_2$ and $PtSn$.

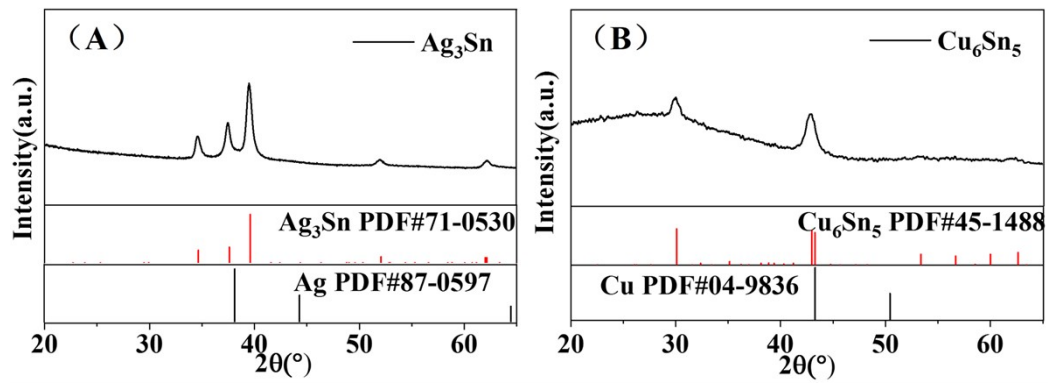


Fig. S7 XRD patterns of (A) Ag_3Sn and (B) Cu_6Sn_5 .

Table S4 The comparison of EOR performance between Pt₃Sn, PtSn, PtSn₂, PtSn₄, and commercial Pt/C. The specific activity of samples and their corresponding peak potential are listed.

EOR performance	Pt/C	Pt ₃ Sn	PtSn	PtSn ₂	PtSn ₄
Peak potential / V vs. SCE	0.656	0.665	0.629	0.613	0.612
ECSA/ m ² g ⁻¹	67.1	57.6	34.8	30.2	30.9
Specific activity/ mA cm ⁻²	1.07	1.09	2.30	2.11	1.78

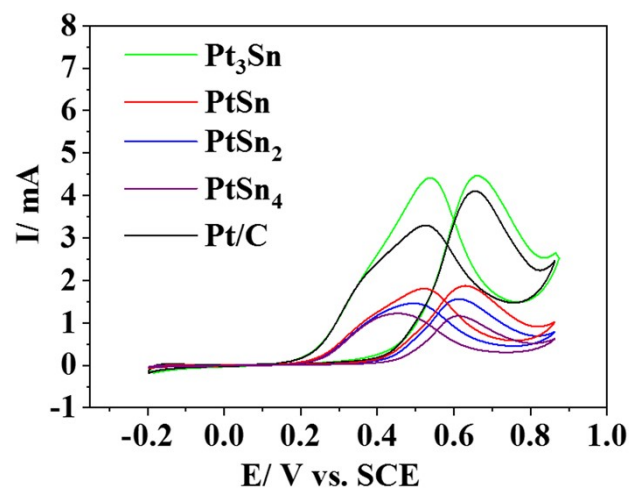


Fig. S8 Electrocatalytic activity current for EOR.

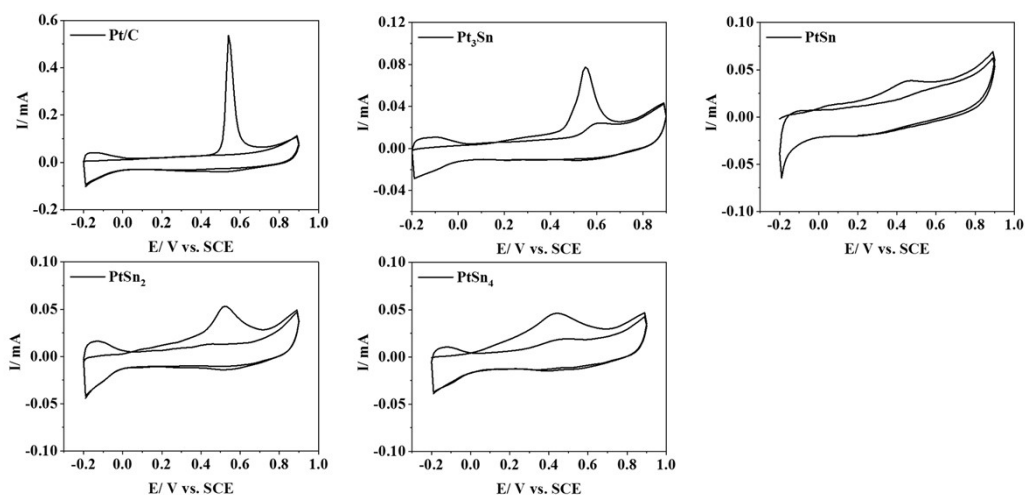


Fig. S9 CO stripping curves of different catalysts. CO stripping curves of (A) commercial Pt/C, (B) Pt₃Sn, (C) PtSn, (D) PtSn₂, and (E) PtSn₄. In the case of Pt_xSn_y, -0.2 V vs. SCE was applied in a CO-saturated 0.5 M H₂SO₄ solution and then N₂ was purged into the electrolyte, followed by a CO stripping cyclic voltammetry curve from -0.2 V vs. SCE to 0.9 V vs. SCE (Method 2). The intensity of the CO stripping peak is higher than the data obtained through Method 1, as shown in the figure. The CO stripping curve onset potentials of PtSn, PtSn₂, and PtSn₄ start from about 0 V vs. SCE, earlier than that of Pt₃Sn and commercial Pt/C, indicating weaker binding energy between PtSn, PtSn₂, and PtSn₄ and CO.

Table S5 Summarization of Sn 3d and Pt 4f peaks from deconvoluted XPS spectra (Fig. 5 (E-F)).

The XPS peaks of Sn 3d and Pt 4f					
Sn	E 3d _{3/2} /eV	E 3d _{5/2} /eV	Pt	E 4f _{5/2} /eV	E 4f _{7/2} /eV
PtSn ₄	487.2	495.7	PtSn ₄	72.5	75.9
PtSn ₄	485.5	494.0	PtSn ₄	73.6	76.8
PtSn ₄	-	-	PtSn ₄	71.6	74.9
PtSn ₂	487.2	495.7	PtSn ₂	72.2	75.6
PtSn ₂	486.1	494.6	PtSn ₂	73.4	76.8
PtSn	486.7	495.2	PtSn	71.7	75.1
PtSn	485.9	494.4	PtSn	72.3	75.6
Pt ₃ Sn	486.9	495.3	Pt ₃ Sn	71.9	75.2

Table S6 The comparison of EOR specific activity and stability between our work and some Pt_xSn_y alloys for EOR in recent works.

Catalyst	ECSA / m ² g ⁻¹	Specific activity / mA cm ⁻²	Peak potential	Stability	Referenc e
Pt ₁ Sn ₃ alloy NWS	0.340	0.35 @ 0.600 V vs. RHE	-	0.600 V vs. RHE 3600 s decrease from 0.500 mA cm ⁻² to 0.200 mA cm ⁻²	1
PtSn ₃ alloy	32.0	1.25@ 0.9 V vs. RHE	-	0.500 V vs. RHE 500 s decrease from 0.300 mA cm ⁻² to 0.0500 mA cm ⁻²	2
Pt ₇₀ Sn ₃₀ intermetallic	13.0	1.41@ 0.350 V vs. Ag/AgCl	-	0.350 V vs. Ag/AgCl 3600 s decrease from 1.50 mA cm ⁻² to 0.250 mA cm ⁻²	3
PtSn alloy	-	0.8@ 0.920 V vs. RHE	0.920 V vs. RHE	0.500 V vs. RHE 600 s decrease from 0.15 mA cm ⁻² to 0.005 mA cm ⁻²	4
PtRhSn alloy	2.65	1.78 @ 0.600 V vs. Ag/AgCl	-	0.350 V vs. Ag/AgCl 300 s decrease from 1.50 mA cm ⁻² to 0.220 mA cm ⁻²	5
PtSn nanoparticle	-	0.70 @ 0.920 V vs. RHE	0.920 V vs. RHE	0.5 V vs. RHE 600 s decrease from 0.17 mA cm ⁻² to 0.004 mA cm ⁻²	6
Our work (PtSn)	34.8	2.30@ 0.629 V vs. SCE		0.500 V vs. SCE 3600 S decrease from 1.90 mA cm ⁻² to 0.322 mA cm ⁻²	
Our work (PtSn ₄)	30.9	1.78@ 0.612 V vs. SCE		0.500 V vs. SCE 3600 S 1.30 mA cm ⁻² , to 0.198 mA cm ⁻²	

Notes and references

- 1 L. Li, H. Liu, C. Qin, Z. Liang, A. Scida, S. Yue, X. Tong, R. R. Adzic and S. S. Wong, Ultrathin Pt_xSn_{1-x} Nanowires for Methanol and Ethanol Oxidation Reactions: Tuning Performance by Varying Chemical Composition, *ACS Appl. Nano Mater.*, 2018, **1**, 1104-1115.
- 2 R. Rizo, R. M. Arán-Ais, E. Padgett, D. A. Muller, M. J. Lázaro, J. Solla-Gullón, J. M. Feliu, E. Pastor and H. D. Abruña, Pt-Rich_{core}/Sn-Rich_{subsurface}/Pt_{skin} Nanocubes As Highly Active and Stable Electrocatalysts for the Ethanol Oxidation Reaction, *J. Am. Chem. Soc.*, 2018, **140**, 3791-3797.
- 3 W. Du, G. Yang, E. Wong, N. A. Deskins, A. I. Frenkel, D. Su and X. Teng, Platinum-Tin Oxide Core-Shell Catalysts for Efficient Electro-Oxidation of Ethanol, *J. Am. Chem. Soc.*, 2014, **136**, 10862-10865.
- 4 R. Rizo, M. Jesus Lazaro, E. Pastor and G. Garcia, Spectroelectrochemical Study of Carbon Monoxide and Ethanol Oxidation on Pt/C, PtSn(3:1)/C and PtSn(1:1)/C Catalysts, *Molecules*, 2016, **21**.
- 5 N. Erini, R. Loukrakpam, V. Petkov, E. A. Baranova, R. Z. Yang, D. Teschner, Y. H. Huang, S. R. Brankovic and P. Strasser, Ethanol Electro-Oxidation on Ternary Platinum-Rhodium-Tin Nanocatalysts: Insights in the Atomic 3D Structure of the Active Catalytic Phase, *ACS Catal.*, 2014, **4**, 1859-1867.
- 6 R. Rizo, D. Sebastián, M. J. Lázaro and E. Pastor, On the design of Pt-Sn efficient catalyst for carbon monoxide and ethanol oxidation in acid and alkaline media, *Appl. Catal., B*, 2017, **200**, 246-254.
- 7 J. Ding, L. Bu, S. Guo, Z. Zhao, E. Zhu, Y. Huang and X. Huang, Morphology and Phase Controlled Construction of Pt-Ni Nanostructures for Efficient Electrocatalysis, *Nano Lett.*, 2016, **16**, 2762-2767.